ARTICLE IN PRESS

Available online at www.sciencedirect.com

ScienceDirect

Advances in Space Research xxx (2016) xxx–xxx

ADVANCES IN SPACE RESEARCH (a COSPAR publication)

www.elsevier.com/locate/asr

Science case for the Asteroid Impact Mission (AIM): A component of the Asteroid Impact & Deflection Assessment (AIDA) mission

Patrick Michel [a,*], A. Cheng [b], M. Küppers [c], P. Pravec [d], J. Blum [e], M. Delbo [a], S.F. Green [f], P. Rosenblatt [g], K. Tsiganis [h], J.B. Vincent [i], J. Biele [j], V. Ciarletti [k], A. Hérique [l], S. Ulamec [j], I. Carnelli [m], A. Galvez [m], L. Benner [n], S.P. Naidu [n], O.S. Barnouin [b], D.C. Richardson [o], A. Rivkin [b], P. Scheirich [d], N. Moskovitz [p], A. Thirouin [p], S.R. Schwartz [a], A. Campo Bagatin [q], Y. Yu [a]

[a] *Laboratoire Lagrange, Université Côte d'Azur, Observatoire de la Côte d'Azur, CNRS, CS 34229, 06304 Nice Cedex 4, France*
[b] *JHU/APL, USA*
[c] *ESA/ESAC, Spain*
[d] *Ondrejov Obs., Czech Republic*
[e] *TU Braunschweig, Germany*
[f] *Open University, UK*
[g] *Royal Observatory of Belgium, Belgium*
[h] *Aristotle University of Thessaloniki, Greece*
[i] *Max-Planck Institute, Göttingen, Germany*
[j] *German Aerospace Center, DLR, Cologne, Germany*
[k] *UVSQ (UPSay), UPMC (Sorbonne Univ.), CNRS/INSU, LATMOS-IPSL, Guyancourt, France*
[l] *Univ. Grenoble Alpes, IPAG, CNRS, IPAG, Grenoble, France*
[m] *ESA/Hq, Paris, France*
[n] *JPL, Pasadena, USA*
[o] *Univ. Maryland, College Park, USA*
[p] *Lowell Observatory, Flagstaff, USA*
[q] *Universidad de Alicante, Spain*

Received 29 October 2015; received in revised form 25 February 2016; accepted 19 March 2016

Abstract

The Asteroid Impact & Deflection Assessment (AIDA) mission is a joint cooperation between European and US space agencies that consists of two separate and independent spacecraft that will be launched to a binary asteroid system, the near-Earth asteroid Didymos, to test the kinetic impactor technique to deflect an asteroid. The European Asteroid Impact Mission (AIM) is set to rendezvous with the asteroid system to fully characterize the smaller of the two binary components a few months prior to the impact by the US Double Asteroid Redirection Test (DART) spacecraft. AIM is a unique mission as it will be the first time that a spacecraft will investigate the surface, subsurface, and internal properties of a small binary near-Earth asteroid. In addition it will perform various important technology demonstrations that can serve other space missions.

The knowledge obtained by this mission will have great implications for our understanding of the history of the Solar System. Having direct information on the surface and internal properties of small asteroids will allow us to understand how the various processes they undergo work and transform these small bodies as well as, for this particular case, how a binary system forms. Making these measurements from up close and comparing them with ground-based data from telescopes will also allow us to calibrate remote observations and improve our data interpretation of other systems. With DART, thanks to the characterization of the target by AIM, the mission will be

* Corresponding author. Tel.: +33 4 92 00 30 55; fax: +33 4 92 00 31 21.
E-mail address: michelp@oca.eu (P. Michel).

http://dx.doi.org/10.1016/j.asr.2016.03.031

Please cite this article in press as: Michel, P., et al. Science case for the Asteroid Impact Mission (AIM): A component of the Asteroid Impact & Deflection Assessment (AIDA) mission. Adv. Space Res. (2016), http://dx.doi.org/10.1016/j.asr.2016.03.031

the first fully documented impact experiment at asteroid scale, which will include the characterization of the target's properties and the outcome of the impact. AIDA will thus offer a great opportunity to test and refine our understanding and models at the actual scale of an asteroid, and to check whether the current extrapolations of material strength from laboratory-scale targets to the scale of AIDA's target are valid. Moreover, it will offer a first check of the validity of the kinetic impactor concept to deflect a small body and lead to improved efficiency for future kinetic impactor designs.

This paper focuses on the science return of AIM, the current knowledge of its target from ground-based observations, and the instrumentation planned to get the necessary data.

Keywords: Planetary defense; Near-Earth asteroids; Asteroid impact hazards; Kinetic impactor; Binary asteroids

1. Introduction

This paper describes the science rationale for the European Space Agency's Asteroid Impact Mission (AIM), either as a standalone mission or as an international cooperation with the NASA Double Asteroid Redirection Test (DART; see the companion paper by Cheng et al. (2016), a mission under study by the Johns Hopkins Applied Physics Laboratory with support from NASA Goddard Space Flight Center, NASA Johnson Space Center, and the Jet Propulsion Laboratory). The combined ESA–NASA mission (Cheng et al., 2015) is called the Asteroid Impact & Deflection Assessment (AIDA). The AIM mission is going through a phase A/B1 study, beginning March 2015 and ending September 2016. The NASA Phase A study of the DART mission began in the fall of 2015 and will end in the summer of 2016. AIDA will be the first test ever to use a kinetic impactor to deflect an asteroid. The AIM/AIDA target is the secondary component of the binary NEA (65803) Didymos (1996 GT). The AIM launch window is October/November 2020, arriving at Didymos in April 2022. DART is planned for launch in December 2020 with impact in late September 2022 when Didymos will be within 0.1 AU of the Earth and observable with small ground-based telescopes. AIM will measure physical and dynamical properties of the Didymos system, releasing a lander and CubeSat payloads before the DART impact, and determine any changes that result from the impact. This paper and the companion paper (Cheng et al., 2016) present the science rationales for the AIM and DART missions, as formulated for the phase A studies.

Several international reports have recommended that a demonstration be undertaken to alter the orbital course of an asteroid (e.g., the white papers of the International Academy of Astronautics (IAA) Planetary Defense Conference 2013 and 2015) due to its scientific and technological interest. The Don Quijote mission study, performed by ESA in 2002–2007, had the objective of demonstrating the ability to modify the trajectory of an asteroid using a kinetic impactor and to observe the consequent change in its orbit, as well as any physical changes, from an observing spacecraft. The kinetic impactor is one of the main concepts under consideration to deflect asteroids of up to a few hundred meters in size. However, the magnitude of the resulting deflection is highly uncertain, owing to the poorly understood contribution of recoil momentum from impact ejecta. An understanding of impact dynamics and fragmentation processes, over a wide range of physical scales, is essential to address many fundamental questions of planetary science as well as a wide variety of technological problems. Several studies are underway to improve our understanding of these processes through numerical modeling, but confirmation of the validity of model results relies on verification with laboratory impact experiments at very small (centimeter) scales. So far, we do not know whether our assumptions to extrapolate our knowledge at laboratory scale to the scale of the impact planned with AIDA are valid, and this knowledge is essential to use these extrapolations for other cases. Moreover, the efficiency of a mitigation strategy highly depends on the physical properties of the asteroid target (Michel, 2013). In particular, the deflection efficiency of a kinetic impactor depends on the asteroid subsurface and internal structures (e.g., Holsapple and Housen, 2012; Jutzi and Michel, 2014), and so far no direct measurement of these properties has been performed on any asteroid. In fact, the physical characterization of a near-Earth asteroid (NEA) as well as understanding how it responds to an impact are crucial in order to fully evaluate the impact event and to address various scientific problems in planetary science. Furthermore, a number of technologies must be demonstrated for this purpose, which can also serve other interplanetary missions and objectives. AIM is specifically designed to address both technological and scientific aspects of impact mitigation. The DART mission includes both the artificial projectile equipped with an imager, and ground-based measurements of the deflection. The impact energy of DART, assuming 300 kg impacting at 7 km/s, will be 1.8 tons of TNT equivalent energy. The AIM mission will provide the first complete view of an asteroid-scale impact ever obtained, including detailed knowledge of the impact conditions prior to DART's impact, and a clear view of the consequences of the impact, including in situ measurements of key physical properties, such as surface, subsurface and internal structures of the target body. The AIDA mission, with both DART and AIM, offers the possibility of detailed interpretation of the deflection

Please cite this article in press as: Michel, P., et al. Science case for the Asteroid Impact Mission (AIM): A component of the Asteroid Impact & Deflection Assessment (AIDA) mission. Adv. Space Res. (2016), http://dx.doi.org/10.1016/j.asr.2016.03.031

measurement and allows for direct comparison with numerical modeling efforts (e.g., Jutzi and Michel, 2014).

AIM has several objectives. First, it will demonstrate, at a low cost for a deep-space mission, technologies related to autonomous navigation, optical communication, on-board resources management, close proximity operations, asteroid microlanders, and deep-space intersatellite networks. Second, AIM will characterize for the first time in detail a binary asteroid, allowing us to better understand the geophysical properties of small asteroids (diameter on the order of a few 100 m), as well as the formation and properties of these systems that represent ≈15% of the NEA population (Margot et al., 2015; Walsh and Jacobson, 2015). Finally, AIM will demonstrate technologies required by a simple monitoring spacecraft, and establish the suitability of binary asteroids for future exploration and asteroid deflection tests.

Both AIM and AIDA address issues that interest several communities, including scientists and engineers working on impact physics, planetary science, seismology, geophysics (surface and internal properties), dynamics, mineralogy and resources, spectral and physical properties of small bodies, low-gravity environments, impact mitigation, and human exploration.

In the following, we present the science topics that will be addressed by AIM, both as a standalone mission and within AIDA, as well as the current knowledge of the environment (i.e., main target's properties) of this mission based on observations and numerical modeling.

2. Scientific motivations

2.1. Knowledge resulting from AIM as a standalone mission

Although AIM is a technology demonstration, an important by-product of the mission will be to enhance drastically our scientific knowledge of small asteroids. This mission is relevant to many aspects of Solar System science, including gaining new insights on granular mechanics in low gravity environments, impact cratering, seismic processes, and thermal properties and processes. It will also greatly inform mitigation techniques, human exploration, and resource utilization strategies (Fig. 1).

The main scientific objectives of the AIM mission are:

- to characterize the mass, size, detailed morphology, and density of the natural satellite of a binary asteroid;
- to determine the dynamical properties of the binary system;
- to determine the surface and sub-surface properties of the natural satellite of a binary asteroid;
- to determine the internal structure of the natural satellite of a binary asteroid;
- to determine the thermophysical properties of the natural satellite of a binary asteroid.

2.1.1. Solar System and binary asteroid science gain

Asteroids are thought to be leftover planetesimals that are closely related to the precursor bodies that formed both the terrestrial planets and the cores of the giant planets. In the last decade, ground-based and spacecraft observations, as well as numerical modeling of small asteroids, have drastically changed our understanding of these bodies (e.g., Michel et al., 2015). Almost all asteroids that we observe today, whether they have a primitive or more evolved composition, are the products of a complex history involving the accretion process as well as one or several episodes of catastrophic disruption and space weathering. Both numerical models and spacecraft images indicate that most NEAs are covered with some sort of regolith (e.g., Murdoch et al., 2015) and are *rubble piles* (Campo et al., 2001; Michel et al., 2001; Fujiwara et al., 2006), i.e., aggregates made of boulders or particles down to gravel or dust sizes,

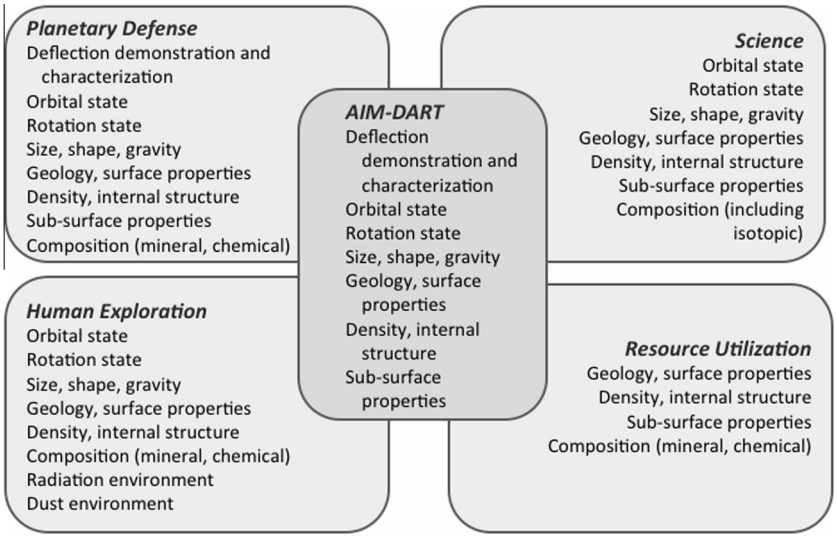

Fig. 1. The knowledge from AIM and AIDA will be relevant to several disciplines.

Please cite this article in press as: Michel, P., et al. Science case for the Asteroid Impact Mission (AIM): A component of the Asteroid Impact & Deflection Assessment (AIDA) mission. Adv. Space Res. (2016), http://dx.doi.org/10.1016/j.asr.2016.03.031

although the actual internal structure of such bodies is still unknown. The detailed properties of asteroid regoliths are still unknown except for two NEAs, (433) Eros and (25143) Itokawa, that have been visited by spacecraft (the NASA NEAR-Shoemaker and the JAXA Hayabusa missions) although even for those cases some characteristics are still not well understood. In fact, asteroid surfaces, which evolve in very-low-gravity environments, are subject to various kinds of processes, including space weathering, impacts, seismic phenomena, regolith migration, and segregation (Murdoch et al., 2015). Some NEAs may be transformed into double systems (binaries) when their rotational rate exceeds the threshold above which material can fly away and potentially form a small satellite (e.g., Walsh and Jacobson, 2015). Small asteroids thus undergo substantial physical evolution, and yet the geophysics and mechanics of these processes are still a mystery. This is at least partly due to a lack of scientific data, both on the mechanical properties of small asteroids, with their very unique micro-gravity environments, and on their subsurface and global geophysics. Direct interaction is the only way to determine the detailed mechanical properties of an asteroid surface and to measure how it responds to an external force. Our knowledge of asteroid geophysics and of aggregate mechanics in micro-gravity environments is thus still very restricted. Moreover, in such low-gravity environments, physical processes caused by forces other than gravity, in particular van der Waals and electrostatic forces, may play a very important role in the mechanical behavior of a small asteroid (Scheeres et al., 2010). Indeed, such forces have been invoked as necessary to retain regolith on the small, fast-spinning rubble-pile asteroid (29075) 1950 DA, where gravity alone is insufficient ((Rozitis et al., 2014; Gundlach and Blum, 2015), who derive cohesive strengths of $64 + 12/-20$ Pa and 25–88 Pa, respectively). If one could confirm these effects on an asteroid surface, this would revolutionize our understanding of small bodies.

One fundamental question is: are small asteroids made of boulders, zones with voids, or smaller components from gravel to dust down to their center? The long history of discussion of this topic is reflected by the large number of publications addressing it (e.g., Britt et al., 2002; Richardson et al., 2002; Consolmagno et al., 2008). Answering this question will allow us to trace back Solar System history from the accretion of these bodies to their current internal and surface properties. An understanding of the mechanical properties of an asteroid and its response to external actions is also crucial for the design of mitigation technologies to deflect hazardous asteroids as well as to prepare future human exploration of asteroids. It is thus time to explore the internal structure and physical properties of one of them.

AIM will target the moon of the binary NEA Didymos (see Section 5.1), but global measurements will also be performed of the primary, which will frequently find itself in the field of view of the instruments expected to fly on AIM (see Section 4). AIM's characterization of both the primary and secondary will significantly improve our knowledge of the physical and compositional properties of a component of the binary NEA population. In addition, the formation of small binaries is still a matter of debate, although several scenarios have been proposed to explain their existence and observed frequency. In particular, rotational disruption of an NEA, assumed to be an aggregate, as a result of spin-up above the fission threshold due to the YORP effect has been shown to be a mechanism that can produce binary asteroids with properties that are consistent with observations (e.g., Walsh and Jacobson, 2015). These properties include the oblate spheroidal shape of the primary, the size ratio of the primary to the secondary, and the circular equatorial secondary orbit. Mass shedding from the primary has been shown to reproduce those properties (Walsh et al., 2008, 2012), giving constraints to the internal structure of the progenitor. Other fission scenarios have been proposed that imply different physical properties of the binary and its progenitor (Jacobson and Scheeres, 2011). Binary formation scenarios therefore place constraints on, and implications for, the internal structure of these objects.

AIM provides us with the first opportunity to directly measure the internal structure of an asteroid to distinguish between a rubble pile with large coherent segments and a rubble pile with small-scale components. These measurements will also allow us to constrain the role of macro- vs. micro-porosity. Combined, these results will lead to new insight in understanding the formation of a binary.

The binary nature of the target allows determination of certain parameters of the target during the mission planning and design phases as the sizes, total mass, and orbit pole direction of the system can be estimated from Earth-based observations. This knowledge will reduce the time required for initial characterization before entering into bound orbits.

The rendezvous of AIM with Didymos will thus allow scientific investigation of the fascinating geology and geophysics of asteroids. For example, precise measurements of the mutual orbit and rotation state of both components can be used to probe higher-level harmonics of the gravitational potential, and therefore internal structure. In addition, the mission provides a unique opportunity to study the dynamical evolution driven by the YORP/Yarkovsky thermal effects. The measurements of the thermal properties of the target and its surface temperature distribution are important in this respect, because they affect the orbital and spin-state evolution of the object via the Yarkovsky and YORP effects, respectively (Vokrouhlický et al., 2015). In particular, the thermal inertia, the resistance of a material to temperature change, dictates the strength of the Yarkovsky effect on the asteroid. The Yarkovsky effect is responsible for the dispersion of the members of asteroid families, the delivery of small asteroids and meteoroids from the main belt into dynamical resonance zones capable of transporting them to Earth-crossing orbits, and the orbital evolution of potentially hazardous asteroids (see Vokrouhlický et al. (2015), and

Please cite this article in press as: Michel, P., et al. Science case for the Asteroid Impact Mission (AIM): A component of the Asteroid Impact & Deflection Assessment (AIDA) mission. Adv. Space Res. (2016), http://dx.doi.org/10.1016/j.asr.2016.03.031

references therein). The value of the thermal inertia can also be used to determine the nature of the soil of the asteroid, e.g., the typical size (Gundlach and Blum, 2013) and degree of cementation (Piqueux and Christensen, 2009a, b) of the particles of the soil, which constitute the so-called asteroidal regolith. Regolith informs us about the geological processes occurring on asteroids (Murdoch et al., 2015), such as impacts (Barnouin et al., 2008), micrometeoroid bombardment (Hörz and Cintala, 1997), and thermal cracking (Delbò et al., 2014). AIM will provide a direct link between thermal inertia observations and surface physical properties measured in situ of a small binary component.

AIM will thus allow us to address fundamental questions, such as:

- What are the surface and subsurface structures of asteroid satellites and how does an asteroid's surface relate to its subsurface?
- What are the geophysical processes that drive binary asteroid formation?
- What are the strength and thermal properties of a small asteroid's surface?
- What is the cohesion within an aggregate in microgravity?
- What are the physical properties of the regolith covering asteroid surfaces and how does it react dynamically to external processes, such as the impact of a surface package?
- What is the link between thermal inertia and actual surface properties?
- What is the internal structure of a small binary component?

2.1.2. Mitigation science

Small bodies continue to shape planetary surfaces throughout the Solar System via collisions. Roughly 50 to 100 tonnes of material fall on the Earth every year. However, much larger objects lurk nearby, astronomically speaking: nearly 1000 objects with a diameter equal to or greater than 1 km are classified as NEAs, with perihelia of 1.3 AU or less. Impacts with objects of that size, which would result in civilization-threatening effects, are thought to recur on roughly million-year timescales. The population of NEAs with a diameter equal to or larger than 50 m is modeled to number in the hundreds of thousands. While impacts by 50 m-diameter asteroids may *only* devastate a relatively small region (as for the Tunguska Event in 1908), they also occur much more frequently; we have to expect such impacts on century-to-millennium timescales. The abstract knowledge that small-body impacts on Earth continue to occur to this day became concrete reality for the residents of Chelyabinsk, Russia on Feb. 15, 2013, when the unexpected explosion of a 17–20 m-diameter asteroid over the city released 500 ± 100 kT (equivalent TNT) of energy (e.g., Brown et al., 2013).

Uniquely for natural disasters, destructive impacts can not only be predicted, but also potentially avoided via human action. The United States Congress directed NASA to find and characterize at least 90% of potentially hazardous asteroids (PHAs; NEAs with a minimum orbit intersection distance (MOID) of 0.05 AU or less and an absolute magnitude of $H < 22$, equivalent to ~140 m in diameter or larger), following up on an earlier charge to find 90% of all km-scale NEAs. Surveys to meet this Congressional mandate are under way using ground-based and space-based telescopes, and programmes are in place to characterize the sizes, shapes, rotation periods, compositions (spectral classes), and other properties of NEAs. The Space Situational Awareness (SSA) programme of ESA also contributes to this effort (Koschny and Drolshagen, 2015).

There are several possible ways to deflect an asteroid, although none has yet been demonstrated. The various methods do not need the same amount of information regarding the targets. We indicate below a few examples (see Michel (2013), for more details).

- Kinetic impactor: the aim is to deflect the asteroid by a hyper-velocity impact of an artificial projectile. Surface and sub-surface mechanical properties and porosity are the fundamental parameters that influence the outcome of such a concept. Size/shape properties are also needed for accurate targeting. The influence of target rotation on the kinetic impactor efficiency is poorly understood, so the relevance of its knowledge cannot be assessed yet. As long as the area of the impact (and distance of shock wave attenuation from the impact point) is small compared to the whole body, the full internal structure does not need to be known.
- Gravity tractor: the aim is to use the gravitational force of an artificial satellite positioned nearby to deflect a small asteroid. Mass is the fundamental parameter that is needed for the gravity tractor. Knowledge on shape and rotational properties is also important for proximity operations (especially if the tractor distance to the asteroid needs to be small).
- Deployment of a device: several concepts suggest deployment of a device, such as a solar sail or other tools to deflect an asteroid. Surface and sub-surface mechanical properties are fundamental parameters for such mitigation techniques. A yet missing understanding of how a given surface reacts to a landing in low-g conditions is also required to make sure that the device has an appropriate design.
- Catastrophic disruption: the aim is to fully disrupt the asteroid down to very small pieces. Some knowledge of the full internal structure (and global strength) becomes necessary.
- Surface ablation resulting in a reaction force opposing the ejected/vaporized surface material: composition and thermal properties are needed for mitigation techniques relying on surface ablation.

Please cite this article in press as: Michel, P., et al. Science case for the Asteroid Impact Mission (AIM): A component of the Asteroid Impact & Deflection Assessment (AIDA) mission. Adv. Space Res. (2016), http://dx.doi.org/10.1016/j.asr.2016.03.031

AIM measurements (see Sections 3.1 and 3.2) will provide crucial information that is relevant to these various mitigation techniques.

2.1.3. Human exploration and resource utilization

The preparation of a human mission to an asteroid will rely on our knowledge of asteroid properties, in particular the mechanical properties at the surface and sub-surface, including regolith/dust properties, since the astronaut will interact with the surface, in a low-gravity environment. The presence of potentially hazardous (for an astronaut) moonlets and the amount/behavior of dust produced by an impact (e.g., a micrometeorite) or an astronaut-surface interaction also need to be assessed. Any human mission to an asteroid will require a precursor robotic exploration in order to minimize risks for the astronauts.

The assessment of the feasibility of asteroid resource utilization requires better knowledge of the detailed composition (mineralogy) of asteroids. Surface and sub-surface mechanical properties are also needed for the design of appropriate tools for material extraction.

2.2. Additional knowledge resulting from AIM within AIDA

The implementation of the full AIDA mission will lead to unique information regarding the concept of the kinetic impactor as a deflection tool as well as the impact process itself.

Collisional events are of great relevance in the formation and evolution of planetary systems, including our own Solar System. In the first stages of planetary formation, low-speed collisions between planetesimals and/or dust drive planetary growth by collisional accretion. In the particular case of our Solar System, some energetic events apparently occurred quite early. For instance, the Moon of our Earth is understood to be the product of ejected debris reaccumulated after the impact of a planetesimal with our proto-Earth (e.g., Canup, 2012; Ćuk and Stewart, 2012; Reufer et al., 2012). In later stages, once the planets were formed, relative speeds between small bodies increased as a result of planetary perturbations. Consequently, our Solar System entered a new regime of high impact energy, in which it continues to evolve. In this regime, collisions do not lead to accretion phenomena but rather to disruptive events. Asteroid families in the asteroid main belt between Mars and Jupiter are the tracers of disruptive events of large parent bodies. Meteorites collected on Earth are another indication of collisional activity as they are the remnants of collisions that have taken place mostly in the main belt. As a consequence, collisions have to be seen as representing an important threat against human efforts in space, which in an extreme case could even lead to the destruction of our biosphere. The collisional process is therefore not a second-order problem in the understanding of the past, present, and future history of our Solar System; it is actually at the heart of its formation and evolution.

The scales of the phenomena that are involved in planetary and small body impacts are larger by far than those reached in laboratory impact experiments. Extrapolations by 15 orders of magnitude in mass are necessary to achieve ranges that are relevant to asteroids and planetesimals. Theoretical models of catastrophic collisions try to fill this gap by establishing non-dimensional relationships between the projectile's size, the impact velocity, the target's strength, its density, etc., that are supposed to be valid at all scales, and which are regrouped in scaling laws (see e.g. Holsapple, 1993). These scaling laws are quite successful at relating projectile size to crater size in the cratering regime, so long as the analogy with a point-source-like explosion holds. Nevertheless, such relationships are necessarily idealized, as they assume a uniformity of the process as well as a structural continuity. Consequently, they cannot predict large-scale impact outcomes with a high degree of reliability. In reality, asteroids are complex entities whose impact response may have little to do with the physical behavior of rock material in the laboratory (dominated by their mechanical strength) or large fluidized spheres (dominated by gravity).

Numerical simulations are another approach to studying the collisional process, with some notable successes. It is now possible to simulate an impact with a certain degree of sophistication and reasonable accuracy thanks to dedicated numerical codes (see, e.g., Jutzi et al. (2015), for a review) accompanied by improvements in computer performance. Important problems can now be addressed concerning the physical nature of individual objects with a collisional history, the origin of asteroid families, the formation of planets through collisional accretion, etc. Impact experiments in the laboratory are crucial to validate those numerical models at small scales before they are applied to large-scale events. However, until an experiment at the real scale of an asteroid collision can be performed, the validity of these simulations at large scales will remain highly uncertain, so performing a large-scale experiment is still crucial.

In addition to the knowledge gains resulting from AIM as a standalone mission, if DART produces an impact on the secondary of Didymos, AIM will allow us:

- to provide the initial conditions of the impact experiment, including at the specific location of DART's impact;
- to observe for the first time the outcome of an impact on a small asteroid and determine, e.g., the crater size and morphology as well as the amount, size distribution, and trajectories of ejecta, at a scale that is well beyond what can be done in the laboratory and corresponding to that involved in the formation and evolution of our Solar System;

Please cite this article in press as: Michel, P., et al. Science case for the Asteroid Impact Mission (AIM): A component of the Asteroid Impact & Deflection Assessment (AIDA) mission. Adv. Space Res. (2016), http://dx.doi.org/10.1016/j.asr.2016.03.031

- to document the first high-speed impact experiment (before and after impact) on a small body within the Solar System;
- to interpret the resulting deflection in a way that is impossible if only ground observations were available;
- to verify or refine numerical impact codes that can then be applied with greater confidence to many problems linked to the formation and evolution of our Solar System and to other kinetic impactor studies.

AIM will contribute measurements from which initial conditions of the impact, e.g., the impact angle, can be determined, and will relate the position of the impact point on the target measured by DART to the detailed properties of the whole object. This knowledge is fundamental for our correct interpretation of the momentum transfer efficiency measurement. Moreover, although the deflection is planned to be observed from the ground, AIM will provide much greater accuracy as well as additional information about the binary system behavior after the impact. Since DART's impact speed is close to the average impact speed (5 km/s) between main belt asteroids, and the corresponding impact energy lies in the cratering regime, which is experienced more frequently by an asteroid than a disruptive event, AIM will provide unique knowledge on the impact process in the very conditions of an asteroid environment at a scale that is unreachable in the laboratory. For the first time, AIM will allow testing of hypervelocity impact models and scaling laws at appropriate scale, and provide real data regarding the initial conditions and outcome, in terms of the crater size and morphology, as well as ejecta production and properties.

It can be expected that a cloud of ejecta, as observed by the Deep Impact (NASA) mission (see below), will result from the DART impact and that, subsequently, a prominent crater will be visible. If AIM is to approach the binary after the impact, it may be possible, via comparison with DART images of the surface prior to impact, to observe the ejecta emplacement. However, the highest science return would be achieved by observing the impact directly as it occurs using the AIM spacecraft or a sub-component. From optical observations, the ejecta sizes and velocities versus angular distribution after a high-speed impact can be determined. The size distribution can also give direct information on the target material properties. For instance, a rubble pile with a preferred component size distribution should be reflected in the ejecta size distribution. If an infrared spectrometer were available, the plume temperatures of the impact could be measured directly, provided that the plume is visible from the spacecraft at its safe position. Any instrument will have a sufficiently short exposure time to temporally resolve the transient hot dust, but the uncertainty in the total intensity is too large to guarantee high-signal-to-noise data. These data would yield valuable information to constrain the energy partitioning during a large-scale impact. The precise size and shape of the crater will also be determined after the impact. The DART impact crater diameter has been estimated for four target cases, ranging from strong and non-porous target material to very weak and highly porous material (Cheng et al., 2016). The predicted crater size for the porous target cases ranges from 6.1 to 17 m, consistent with predictions from numerical simulation models (Holsapple and Housen, 2012; Jutzi and Michel, 2014). For instance, for an expected crater diameter of 10 m and the planned minimum image resolution of 1 m in the global post-impact survey, we will obtain a 5% accuracy in crater radius (assuming 1 pixel) and 15% in crater volume. The post-impact survey will also provide the depth/diameter ratio and the global morphology of the crater, which are indicative of sub-surface structural properties. In addition, a comparison of high frequency radar signals before and after impact will indicate any sub-surface structural changes that may occur as a result of the impact. Much higher resolution imaging (≈10 cm) may also be acquired through a close flyby during the post-impact phase.

This information will allow us to verify, compare, and refine our impact modeling tools and scaling laws. Once validated with AIDA, they will then be used with higher confidence to design other similar concepts in the future. This knowledge will also have a wide range of implications in planetary science, as the understanding of the impact response of a small body as a function of impact conditions and physical properties is crucial to estimate its collisional lifetime, the collisional evolution of asteroid populations (when this knowledge is extrapolated to other bodies), and the role of collisions in various phases of our Solar System history, as described above.

So far, the only mission that has performed such an impact is the Deep Impact mission (NASA) on July 4, 2005. The target was a comet, 9P/Tempel 1, 6 km in diameter, i.e., much greater than AIDA's target (160 m in diameter, see Section 5.1), and the resulting crater could not be seen due to obscuration by the unexpectedly large amount of fine ejecta. Moreover, the outcome was possibly influenced by the sublimation of volatiles from the subsurface, which is not expected in the case of AIDA's target. The STARDUST-NExT mission (NASA) visited Tempel 1 much later, in 2011, after the comet passed its perihelion, and tentatively identified a shallow crater and other impact features resulting from Deep Impact (Schultz et al., 2013; Richardson and Melosh, 2013). But there is no clear guarantee that other processes did not affect the crater after such a long time, especially after a passage at close proximity to the Sun. The Hayabusa-2 mission (JAXA), which was successfully launched on December 3, 2014, carries a Small Carry-on Impactor (SCI) that will impact the primitive NEA (162173) 1999 JU3 in 2018. The mass of the copper projectile (2 kg) and its impact speed (2 km s^{-1}) are expected to produce a small crater (order of a few meters) but not to produce a measurable deflection. Therefore AIM will be the only spacecraft that will observe the impact of a projectile in the impact speed regime that is both linked to a deflection technology demonstration and

Please cite this article in press as: Michel, P., et al. Science case for the Asteroid Impact Mission (AIM): A component of the Asteroid Impact & Deflection Assessment (AIDA) mission. Adv. Space Res. (2016), http://dx.doi.org/10.1016/j.asr.2016.03.031

consistent with the average impact speed (about 5 km/s) between asteroids in the main asteroid belt.

A fundamental science return from the AIDA cratering experiment will be the determination of whether the crater forms in the strength or gravity regime, indicating whether material strength or the body's gravity limits growth. This is a highly debated topic that requires experimental data. Given the relatively small size of AIDA's target, it is expected that the crater will form in the strength regime and, if that is the case, the DART impact will offer us a good indication of the material strength of the asteroid surface (Holsapple and Schmidt, 1987). On the other hand, if the crater is found to be gravity-dominated, it will mean that the cohesion of the surface material is extremely small (e.g., Holsapple et al., 2002), less than the cohesion expected from van der Waals forces alone (Scheeres et al., 2010), which will provide interesting information on the mechanical properties of the asteroid.

2.3. Summary of knowledge gain resulting from both concepts

Fig. 1 shows the wide range of objectives that AIM will achieve, as explained in the previous sections. With DART (Cheng et al., 2016), it will also serve planetary defense and Solar System science by participating in the first ever actual deflection demonstration and by measuring the outcome of the impact process at real asteroid scales.

3. AIM goals and associated payload

In this section, we indicate the most relevant physical parameters to be measured and instruments required to address the science topics described in previous sections. The exact requirements for these measurements in terms of precision and accuracy are not provided as they will be refined during the Phase A/B1 study ending in Summer 2016. Fig. 2 shows the sequence of operations planned for AIM to reach its goals.

3.1. Measurements by AIM

Images in the visible, as well as the mass and surface (thermal and material) properties of the secondary of the binary asteroid Didymos, are mandatory outputs of AIM, as they serve all areas indicated in Fig. 1. A surface package will allow us to have highly accurate measurement at a specific location on the asteroid and to better understand the mechanical response of the surface. The surface package will also accommodate one element of a bistatic low-frequency radar instrument, providing unique data on the internal structure of the secondary. Free-flying CubeSats deployed before the DART impact will enhance the science return of the mission through additional distributed observations. A laser communication terminal could also be used as an altimeter, allowing very accurate orbit determination and consequently a better measurement of the masses of the primary and the secondary.

The radio-science experiment (RSE) will be performed using the spacecraft Telemetry, Tracking and Command (TT&C) radio-transponder. Both the laser communication terminal and the RSE will enhance the accuracy of orbit determination and will support a first ever in situ GRavity Experiment (GRE) on a binary system (as already done with RSE for planets, (e.g., Rosenblatt and Dehant, 2010) and for single asteroids, (e.g., Konopliv et al.,

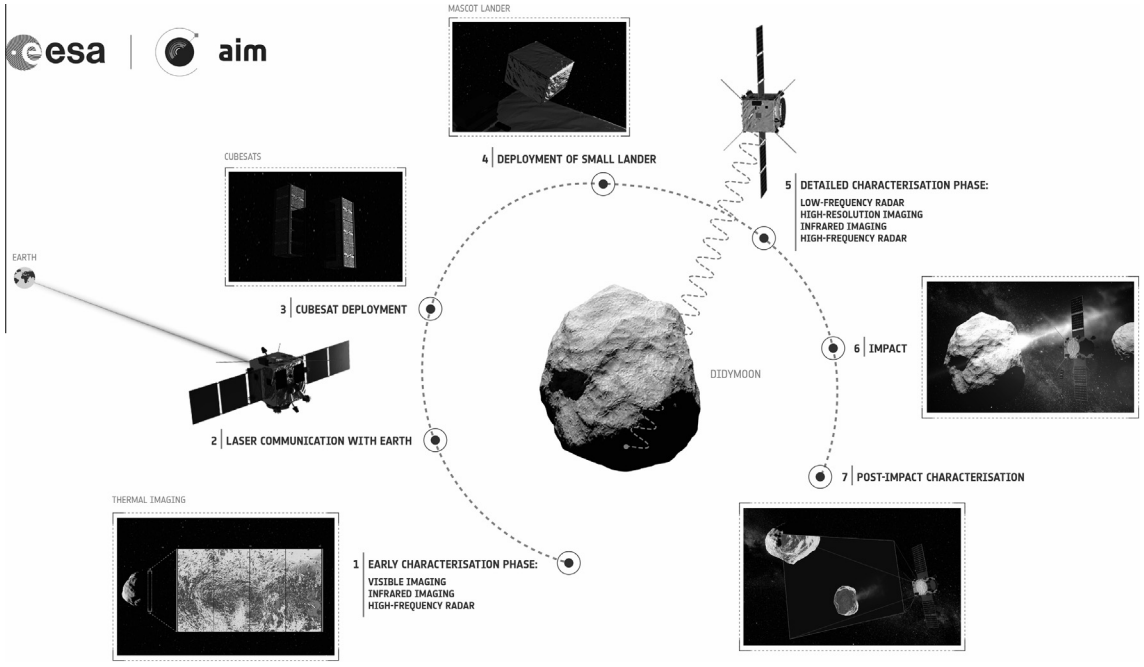

Fig. 2. AIM operations and measurements before and after DART impact.

Please cite this article in press as: Michel, P., et al. Science case for the Asteroid Impact Mission (AIM): A component of the Asteroid Impact & Deflection Assessment (AIDA) mission. Adv. Space Res. (2016), http://dx.doi.org/10.1016/j.asr.2016.03.031

2002)). The RSE will also help to accurately measure the expected orbital change of the system.

A binary offers the possibility of observations of two objects rather than one. Most of the time both the primary and the secondary of Didymos will be in AIM's field of view, so AIM will also measure some physical properties of the primary. In fact, even when getting very close to the secondary, observations of the primary will probably be necessary for navigation purposes. Therefore, global measurements, and most likely also a number of the high-resolution measurements, will be performed for both components. Information on the primary will allow us to improve our understanding of the processes that link the two bodies and provide insight into the binary formation mechanism. In addition, a binary primary could also be the target of a future mission that would greatly benefit from a precursor mission (e.g., for mitigation, resource utilization, or human exploration).

3.2. Measurements by AIM in the framework of the AIDA cooperation mission

The following additional measurements will be performed in the context of AIDA:

- Precise impact conditions (geometry/environment of the impact) of DART to interpret the deflection also measured by ground-based observations.
- Physical properties of the secondary (impacted body) and their modification after impact (i.e., the characterization shall be carried out before and after the impact), the ejecta properties (size/speed), and the crater morphology.Knowledge of the initial conditions and outputs of the impact will provide inputs and a test case for numerical models that can then be refined and used with higher confidence for other cases.
- Orbital properties of the system and their changes after the impact (change in the orbit of the secondary around the primary).

4. AIM baseline payload

To perform the defined measurements, AIM will carry the payload indicated in Table 1. The proposed research objectives, the associated required accuracies and supporting instruments of AIM as a stand-alone mission are indicated in Table 2. In addition, we plan to perform simultaneous ground and space-based measurements (optical, infra-red and radar) that enable the calibration of ground-based observations and their extrapolation to other objects observed from the ground (ground-truth). Other objectives are indicated in Table 3. They are defined to be those objectives that measure properties that are relevant for the combined AIDA (AIM + DART) mission, or enhance the scientific return of a mission to a binary target. The objectives are focused on the secondary of the binary target, unless stated explicitly.

Table 1
AIM baseline payload.

Payload	Acronym
Visual imaging camera	VIS
Monostatic high-frequency radar	HFR
Bistatic low-frequency radar	LFR
Small lander (including low-frequency radar)	MASCOT-2
Thermal infrared imager	TIRI
Optical terminal	OPTEL
CubeSat opportunity payloads	COPINS

VIS is actually part of the spacecraft Guidance, Navigation and Control (GNC) subsystem but it will be used as a remote sensing instrument to provide detailed images of the surface.

Two radar instruments operating at different frequency ranges will allow us to collect for the first time direct information on the subsurface and internal structures of a small asteroid. The high-frequency radar (HFR) will sound the first tens of meters of the regolith of both the primary body and its moon in order to image their structure with a 1-m resolution and detect potential layering and embedded large rocks (Herique, 2015). With a large enough number of acquisition orbits, we will be able to map the spatial diversity of the regolith. The same observation repeated after the DART impact will provide a unique opportunity to probe the impact crater and to detect subsurface changes induced by the impact in order to better model impact/-body mechanical coupling. This step-frequency radar with heritage from WISDOM/Exomars HF operated over a broad frequency bandwidth has a frequency range from 300 MHz up to 3 GHz (Ciarletti et al., 2011). The low-frequency radar (LFR) will be used to probe the deep interior of the secondary body and to characterize its structural homogeneity in order to discriminate monolithic structure versus aggregate, to characterize the size distribution of the constitutive blocks, and to estimate the average complex dielectric permittivity, which relates to the mineralogy and porosity of the constituent material (Herique, 2015). This 60 MHz bistatic radar with a unit on both MASCOT-2 (see below) and the AIM spacecraft is based on CONSERT, the radar on Rosetta and Philae (Kofman, 2007; Kofman et al., 2015). As a secondary objective, both radars will support the determination of the system dynamical state.

MASCOT-2 is a small ($\approx$ 10kg) lander, based on the design of MASCOT (1) which is part of the Hayabusa 2 mission (Jaumann et al., 1999; Ulamec et al., 2014). It will be deployed from the mother spacecraft and land on the secondary. After several bounces and possible re-location by an internal hopping mechanism it will operate for several months on the asteroid surface and provide detailed information about its landing site and the physical properties of the surface material. Besides the lander unit of the LFR, a camera will provide high-resolution images of the

Please cite this article in press as: Michel, P., et al. Science case for the Asteroid Impact Mission (AIM): A component of the Asteroid Impact & Deflection Assessment (AIDA) mission. Adv. Space Res. (2016), http://dx.doi.org/10.1016/j.asr.2016.03.031

Table 2
Research objectives of AIM as a stand-alone mission.

Parameter	Required accuracy	Associated payload
Size, mass, shape, density	• Mass: 10%	Mass from binary orbit, spacecraft tracking (RSE,Optel-D, VIS)
	• Density: 20%	
	Shape accuracy of ≈6% or a few meters	Shape model (VIS), laser altimetry (Optel-D)
Dynamical state (period, orbital pole, spin rate, spin axis)	• Period already known to better than 0.1%	VIS
	• Orbital pole: 5°	
	• Spin rate: 1%	
	• Spin axis: 1°	
Geophysical surface properties, topology, shallow subsurface	• Global surface resolution: 1 m	VIS for surface features
	• Local surface resolution (10% of the surface): 10 cm	
	• Thermal measurement: 20 m resolution	TIRI for surface roughness
	• Subsurface structure and layering: down to 10 m with 1 m resolution, upper ≈2 m with 20 cm resolution	HFR for shallow sub-surface structure
	• Surface compressive strength: within a factor of 3 up to 50 MPa	Accelerometer on MASCOT-2
Deep internal structure	Resolution of interior structure: 30 m	LFR

Table 3
Research objectives of AIM with DART and other objectives.

Parameter	Required accuracy	Associated payload
Full post-impact characterization	Same as pre-impact	All instruments
Primary's surface and sub-surface	Same as for the secondary	VIS, TIRI, HFR, LFR (TBC)
Impact ejecta	Due to the large uncertainties in the properties of the dust cloud, not a driver in requirements on the payload. No accuracy requirements provided	VIS, HFR, TIRI (TBC)
Ambient dust	Due to the large uncertainties in the properties and existence of ambient dust, not a driver in requirements on the payload. No accuracy requirement provided	VIS, TIRI
Chemical and mineral composition of secondary and primary	Spectral resolution: $\lambda/\Delta\lambda = 200$	VIS (TBC), TIRI MASCOT-2 (TBC)

landing area, and accelerometers will interpret the bouncing dynamics. During the DART impact, MASCOT-2 will possibly be able to detect the seismic shock with its accelerometers. Exact timing could give valuable information on the internal structure (from the velocity of p-waves). MASCOT-2 will also serve as a technology demonstrator for asteroid landing and extended operations, powered by a solar generator.

The thermal infrared imager (TIRI) will provide images of the primary and secondary at mid-IR wavelengths, from which the surface temperature distribution, thermal inertia, and surface roughness (at scales smaller than the resolution, but larger than the thermal skin depth of a few cm) can be derived.

The optical terminal (OPTEL) will allow qualification of end-to-end 2-way deep-space optical communication systems for small missions, and will be used as a laser altimeter.

The CubeSat opportunity payloads (COPINS) will consist of the deployment of two 3U CubeSats (or any combination of these units). Its science goal has not been defined yet (five studies of different concepts are currently under way). It will serve to demonstrate deep-space inter-satellite communications for independent CubeSat-based sensors and provide the potential for measurements that are not possible, or deemed too high a risk, for the AIM spacecraft. Also, the combination of AIM, COPINS, and MASCOT-2 will provide a demonstration of inter-satellite link networking between the three components.

The RSE will rely on the spacecraft radio-transponder and on the network of ground-based deep-space antennas. In addition to the laser ranging measurements along the Earth-spacecraft Line-Of-Sight (LoS) direction, it will provide Doppler measurements related to the LoS velocity variations of the spacecraft (and also ranging, although with less accuracy than the laser). Moreover, the RSE can measure the plane-of-sky position of the spacecraft normal to the LoS direction using the radio-telescopes of the VLBI (Very Large Baseline Interferometry) network (Duev et al., 2012). The LoS ranging and the plane-of-sky measurements will help to better constrain the ephemeris of the binary system. The GRE will provide better

Please cite this article in press as: Michel, P., et al. Science case for the Asteroid Impact Mission (AIM): A component of the Asteroid Impact & Deflection Assessment (AIDA) mission. Adv. Space Res. (2016), http://dx.doi.org/10.1016/j.asr.2016.03.031

Table 4
The binary orbit solution of Didymos. 3σ indicates a 99.7% confidence interval. The obliquity refers to the heliocentric orbit.

Nominal orbital pole	$L_{orb} = 310°, B_{orb} = -84°$	
Obliquity	$171° \pm 9°$	3σ
Diameter ratio D_S/D_P	0.21 ± 0.01	
Secondary orbital period P_{orb}	$11.920\ h + 0.004/-0.006\ h$	3σ
Secondary orbital eccentricity	Upper limit: 0.03	3σ
Secondary orbital inclination i_{orb} (assumed)	0°	Primary equatorial coordinates

Table 5
Known dynamical and physical properties of the binary asteroid Didymos. The heliocentric orbital elements are given at epoch 2457000.5 (2014-Dec-09.0), reference: JPL 120 (heliocentric ecliptic J2000); 2015-Jun-04 18:20:59.

Heliocentric semi-major axis	$(1.6444327821 \pm 9.8 \times 10^{-9})$ AU	JPL
Heliocentric eccentricity	$0.383752501 \pm 7.7 \times 10^{-9}$	JPL
Heliocentric inclination (ecliptic)	$(3.4076499° \pm 2.4 \times 10^{-6})°$	JPL
Primary rotation period	(2.2600 ± 0.0001) h	
Distance between component COMs	$(1.18\ +0.04/-0.02)$ km	
Mean diameter of the primary D_P	0.780 km ± 10% (3σ)	PDS, pole sol. 2
Mean diameter of the secondary D_S	(0.163 ± 0.018) km	
Secondary (shape) elongation a_S/b_S and b_S/c_S (assumed)	$1.3 \pm 0.2 > 1$ (assumed: 1.2)	See discussion on shape model
Bulk density of the primary ρ_P	2100 kg m^{-3} ±30%	See text
Total system mass	$5.28 \pm 0.54 \times 10^{11}$ kg	
Mean absolute magnitude (whole system) H	18.16 ± 0.04	
Geometric albedo	0.15 ± 0.04	From D_P, D_S, H
Radar albedo	$0.27 \pm 25\%$	PDS, pole sol. 2

determination of the primary to secondary mass ratio and the moments of inertia of the primary through the measurements of the second-order coefficients of the primary gravity field (namely J_2, dynamical flattening, and C_{22} coefficients). Both measurements will better constrain the interior structure of the system components, i.e., the porosity index and the internal mass distribution, which are key parameters to test several models of formation of the binary system (e.g., Walsh and Jacobson, 2015). The porosity is also a key parameter for risk mitigation as the momentum transfer efficiency of a kinetic impactor highly depends on the porosity (Jutzi and Michel, 2014).

5. AIM environment

5.1. Known target properties

(65803) Didymos (preliminary designation 1996 GT) is an Apollo asteroid (semimajor axis $a > 1$ AU, perihelion distance $q < 1.017$ AU) discovered on April 11, 1996 by *Spacewatch* at Kitt Peak. Its binary nature was discovered with photometric and radar observations obtained shortly after its close approach to Earth (at a minimum distance of 0.048 AU) during the period November 20–24, 2003 (Pravec et al., 2003).

The main physical and dynamical properties of the binary system were derived or constrained from the photometric observations, the radar observations, or their combination. The known parameters of Didymos are summarized in Tables 4 and 5. Note that the only dynamical parameters directly measured by the observations are the orbital period of the secondary around the primary, their orbital separation, the rotation period of the primary and the size ratio of secondary to primary. All other quantities (e.g. system's mass etc) are derived from these measured parameters. In the following, we briefly describe their derivation.

A parameter of critical importance for the determination of many other properties of Didymos is the orientation of the mutual orbital plane of the Didymos components in space, i.e., the pole of the orbital plane on the celestial sphere. Scheirich and Pravec (2009) modeled the photometric data obtained during November 20 to December 20, 2003 (Pravec et al., 2006) and they found two possible solutions for the orbital pole, one prograde and one retrograde. Follow-up observations that were obtained with the 4.3-m Lowell Discovery Channel Telescope on April 13–14, 2015, are consistent with the retrograde solution, but not the prograde one. Though confirmation with additional and higher-quality observations planned for 2017 will be needed, we choose the retrograde pole solution, which is consistent with the 2015 data, in our further analyses. The currently best determined allowed 3σ area for the retrograde orbital pole is shown in Fig. 3. The nominal pole solution is given in Table 4.

For the retrograde pole, Scheirich and Pravec (2009) determined the orbital period to be $11.920 + 0.004/-0.006$ h, the secondary-to-primary mean diameter ratio $D_S/D_P = 0.21 \pm 0.01$ and they constrained the eccentricity to be $\leqslant 0.03$ (the uncertainties and the upper limit

Please cite this article in press as: Michel, P., et al. Science case for the Asteroid Impact Mission (AIM): A component of the Asteroid Impact & Deflection Assessment (AIDA) mission. Adv. Space Res. (2016), http://dx.doi.org/10.1016/j.asr.2016.03.031

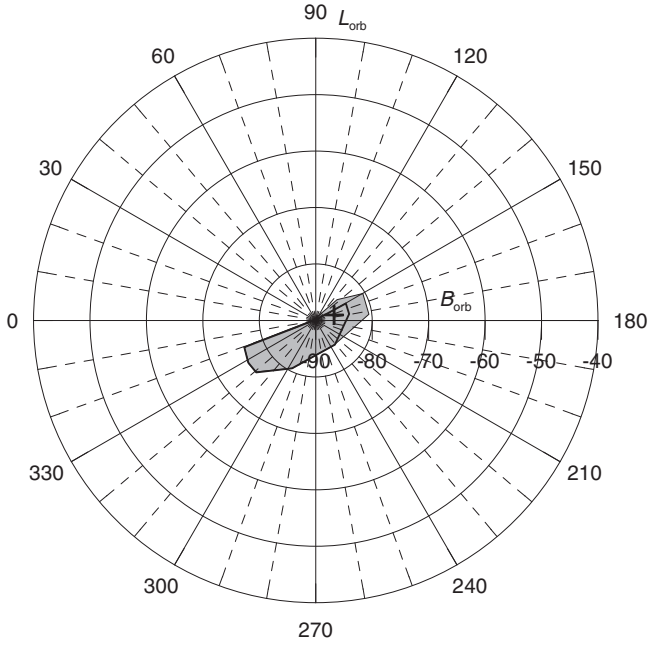

Fig. 3. The allowed (3-σ) area of the retrograde pole of the mutual orbit of Didymos' binary components in ecliptic coordinates. The gray area was derived from the 2003 + 2015 photometric observations. The bold curve is an outline of the area that was further constrained with the modeling refined using the preliminary primary shape model. The + symbol is the south pole of Didymos' heliocentric orbit.

are 3σ). For the retrograde pole, we refined the primary rotation period from the original estimate by Pravec et al. (2006) to $P_P = 2.2600 \pm 0.0001$ h.

Assuming zero inclination of the mutual orbit to the primary's equator, i.e., the primary pole being the same as the orbital pole, Naidu and Benner modeled the Didymos' primary using their 2003 radar observations taken at Goldstone and Arecibo – the best delay-Doppler images had a range resolution of 15 m – and the photometric data for the primary by Pravec et al. (2006). Their preliminary primary shape model is shown in Fig. 4. They obtained a mean diameter (i.e., the diameter of a sphere with the same volume) of $D_P = 0.78$ km with a conservative uncertainty of ±10%. The mean diameter of the secondary, called hereafter *Didymoon* for the sake of simplicity, derived from D_P and D_S/D_P, is $D_S = 0.163 \pm 0.018$ km. Combining the mean diameter values with the system's mean absolute magnitude $H = 18.16 \pm 0.04$ by Pravec et al. (2012), we then obtain Didymos' geometric albedo $p_V = 0.15 \pm 0.04$, which is a typical value for S-type asteroids and therefore consistent with Didymos' S-type classification (see below). The radar albedo of 0.27 (±25%) is consistent with silicates and inconsistent with pure metal. Near-surface roughness is lower than the NEA average and somewhat less than on Eros, Itokawa, and Toutatis.

Didymos is classified as an S-type by de León et al. (2010) based on its 0.4 to 2.5μ spectrum, and as an Xk-type by Binzel et al. (2004) based on a visible spectrum. Fig. 5 shows the spectrum obtained by de León et al. compared with that of two visited NEAs, namely (433) Eros and (25143) Itokawa. S-type asteroids may be associated with L5 and LL5 meteorites.

Fang and Margot (2012) determined the distance between the centers of mass (COMs) of the two bodies, i.e., the semi-major axis $a = 1.18 + 0.04/-0.02$ km and, with the orbital period by Scheirich and Pravec (2009), the total system mass $M_{tot} = (5.3 \pm 0.5) \times 10^{11}$ kg. From the values of the component mean diameters and the total system mass, we obtain a nominal value for Didymos' bulk

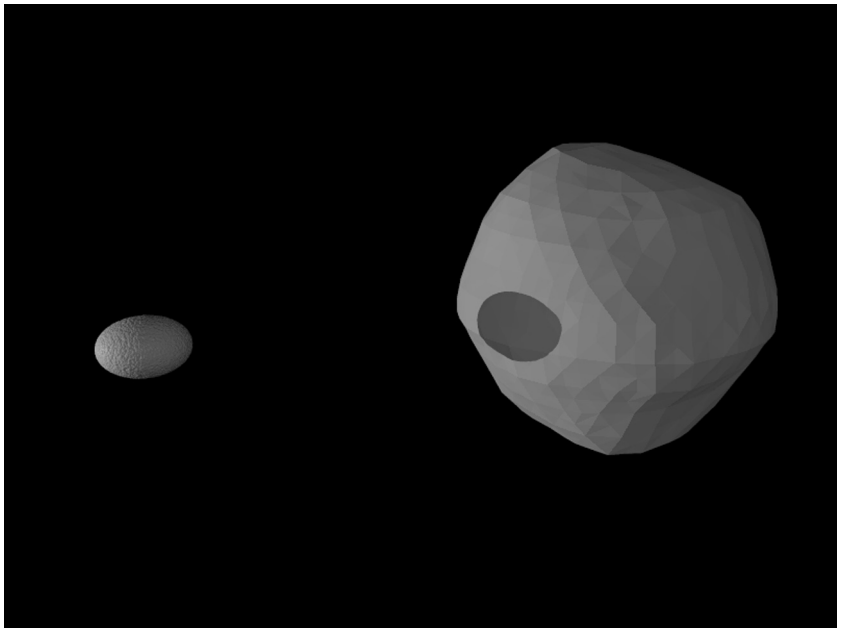

Fig. 4. Preliminary shape model of the primary of Didymos obtained from combined modeling of the radar and photometry data from 2003, shown with Didymoon at scale with assumed ellipsoid axes (see Table 5).

Please cite this article in press as: Michel, P., et al. Science case for the Asteroid Impact Mission (AIM): A component of the Asteroid Impact & Deflection Assessment (AIDA) mission. Adv. Space Res. (2016), http://dx.doi.org/10.1016/j.asr.2016.03.031

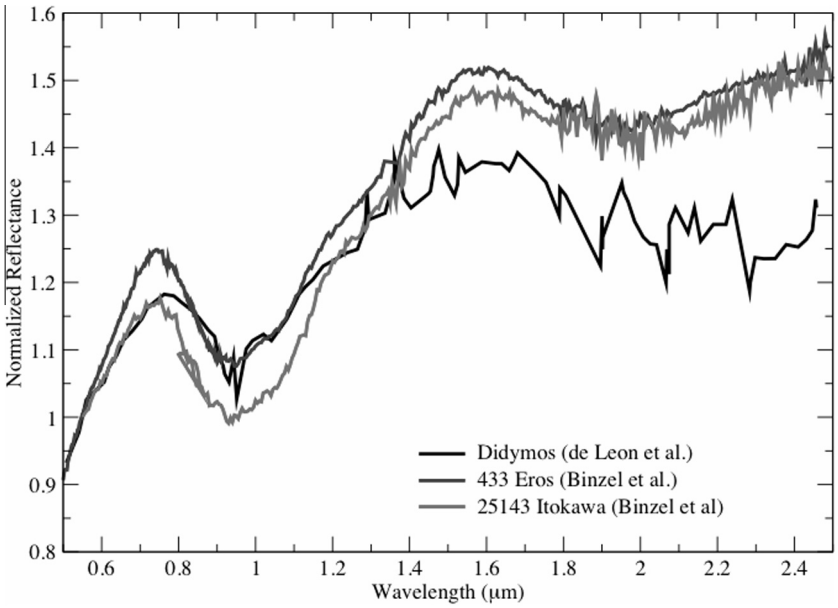

Fig. 5. Spectrum of Didymos (de León et al., 2010), compared with that of two other S-types, namely Eros and Itokawa.

density of 2100 kg m^{-3}, but with a high (conservative) uncertainty of ±30%. A comparison of this bulk density with the density of L-type meteorites, used as meteorite analogs of S-type asteroids (Consolmagno et al., 2008), suggests the asteroid's porosity is ≈45%. Assuming the same density for both components, the secondary-to-primary mass ratio is $M_S/M_P = V_S/V_P = (D_S/D_P)^3 = (0.21 \pm 0.01)^3 = 0.0093 \pm 0.0013$. This shows how small the mass of Didymoon is (about 5×10^9 kg), with respect to that of the primary.

Physical properties of Didymoon other than its mean diameter and mass have not been observationally constrained. Based on data for other asteroid binary systems similar to Didymos (Pravec et al., 2016), we assume that Didymoon is in a 1:1 spin–orbit resonance, i.e., its rotation is synchronous with its revolution around the primary, $P_S = P_{\rm orb}$. Observed radar bandwidths and extents of Didymoon are consistent with this assumption. For modeling purposes, the shape of Didymoon is assumed to be a triaxial ellipsoid with the axis ratios indicated in Table 5. The assumed a_S/b_S is based on the observations of similar systems and on stability arguments (Pravec et al., 2016). The assumed b_S/c_S is based on the observations of similar systems. The rotation state is not constrained by observations and may be unstable (tumbling) for $a_S/b_S \sim 1.4$. The major semi-axis a_S is oriented in the x axis of the corotating frame, i.e., in the direction that connects the COMs of the primary and Didymoon. However, because there may be a small eccentricity, a_S may librate about the line connecting the COMs of the two bodies. Naidu and Margot (2015) estimated that the libration amplitude could be up to 15°. The minor semi-axis c_s is identified with the assumed Didymoon spin direction. The intermediate semi-axis b_S is in the mutual orbit plane, since the obliquity of Didymoon is assumed to be zero. The numerical values of the semi-axes follow from the condition of volume equivalence of an ellipsoid, $a_S \times b_S \times c_S = (D_S/2)^3$, from which $a_S = 0.103$ km. The nominal values of the minor axes are $b_S = 0.079$ km and $c_S = 0.066$ km.

5.2. Unknown target properties

Many properties cannot be determined, or may be very poorly measured, from ground-based observations, although reasonable constraints can be placed on some through modeling. AIM will allow our predictions to be tested.

5.2.1. Main physical properties

Knowing the shapes, masses, spins, and separation of the Didymos components, within uncertainties, it is possible to build numerical models of the Didymos system, treating the components as aggregates of discrete fragments, and test for example the stability of the primary's shape. These studies are currently under way. Preliminary analysis confirms that the primary is close to the critical rotation rate for regolith motion or wholesale shape change. Depending on the actual bulk density of the primary, cohesion may be required to prevent surface motion and/or particle lofting. Indeed, the primary spin is so close to critical that its stability is very sensitive to poorly constrained parameters. Conversely, an assumption of stability may provide constraints on these parameters, including for example the bulk friction angle of the constituent material. The spin limit for the actual shape model, as a function of density and friction angle, will be the subject of a future study.

Further work regarding the modeling of YORP spin-up may provide some additional constraints. In particular, YORP spin-up can lead to migration of material from

Please cite this article in press as: Michel, P., et al. Science case for the Asteroid Impact Mission (AIM): A component of the Asteroid Impact & Deflection Assessment (AIDA) mission. Adv. Space Res. (2016), http://dx.doi.org/10.1016/j.asr.2016.03.031

the pole to the equator, turning an almost spherical object into an oblate spheroid with an equatorial ridge (Walsh et al., 2008). A better understanding of this process can allow the determination of the possible evolution of the shape of an object as a function of its thermal properties and other relevant physical/dynamical properties.

The mass and possibly size of Didymoon, and consequently the density difference between the primary and Didymoon, will not be known in advance with high accuracy; so far we assume that both components have the same bulk density (see Section 5.1). The same holds true regarding detailed surface properties as well as any knowledge of the internal structure. However, based on our understanding of binary formation by YORP spin-up, it is likely that both components of Didymos are gravitational aggregates (Walsh et al., 2008; Walsh et al., 2012), even if cohesion may play a role. In particular, Didymoon could be formed by reaccumulation of small pieces escaping the primary during YORP spin-up. The primary may also be richer in regolith at its equator as a result of this process (see next section).

5.2.2. Surface properties

The surface may be covered by regolith and/or rocky material. The cumulative number of rocks with diameter greater than or equal to a given diameter D (in m), per square meter, is given by $N(D)$.

The differential size frequency distribution (SFD) of surface rocks is frequently observed to follow a power law described by $dN = KD^q dD$ where dN is the number of boulders per unit area in the diameter range between D (typically, the long diameter of an ellipse fitted to the image) and $D + dD$, and where K and q (assuming $-4.5 < q < -3$) are constants of the power-law. The cumulative distribution $N_c(D > D_c)$ is the integral of the differential distribution, or:

$$N_c(D > D_c) = \int_{D_c}^{\infty} KD^q dD = \frac{-K}{q+1} D_c^{q+1} = cD^p$$

$$p = q + 1, \quad c = -K/(q+1) = -K/p$$

Note that the measurement error of any N in a bin is given by $\sqrt{N}$ (Poisson statistics). However, such a power law holds only over limited ranges of D and leads to unphysical results for D tending to 0 and for very large D.

Nothing is actually known observationally about the rock size distribution on Didymoon. However, we can attempt some predictions based on current knowledge, as this is needed to establish baseline surface property expectations in the mission design. We assume the cumulative size distribution as given by a power law with an exponent p between -2 and -3.5 (as observed for many bodies and consistent with theoretical expectations) and define two extreme cases, *smooth* vs. *rocky*. These were derived from the rock size distribution on Itokawa (Mazrouei et al., 2014); for rock sizes > 2 m, and scaled to unit area (using Itokawa's surface area of 0.40403 km^2; (Gaskell et al., 2008)). We define 'pebbles', 'cobbles' and 'boulders' as surface particles with size ranges in intervals of 4 mm–6.4 cm, 6.4 cm–2.56 m, and >2.56 m, respectively (Wentworth, 1922); 'gravel' includes all of them. Pebbles are not regarded as rocks but rather as part of the regolith. Very large boulders can be modeled as part of the shape model.

The nominal surface of Didymoon is 85660 m^2 (surface of the nominal triaxial ellipsoid).

5.2.3. Thermal properties

Knowledge of thermal properties is important for the science return of the mission and the design of the spacecraft. For instance, the value of the thermal inertia — $\Gamma = \sqrt{\kappa\rho C}$, where κ, ρ, and C are the thermal conductivity, the density, and the heat capacity of the surface regolith, respectively — controls the surface temperature distribution, which in turn governs the non-gravitational perturbations (Yarkovsky effect) that act on the asteroid's trajectory. Moreover, estimates of the surface temperature and its variations are required for the design of the lander MASCOT-2. In effect, during the near-surface operation of the spacecraft, all instruments receive heat from the surface of the asteroid. It is thus paramount to take into account the potentially hot surface of the asteroid, during these phases of the mission.

Published values of Γ for NEAs of size and composition similar to Didymos (Delbò et al., 2015) are between 400 and 1000 J m^{-2} s$^{-0.5}$ K^{-1}. Unfortunately, the thermal inertia of Didymos may not be known before its 2022 close approach to Earth and AIM's visit, since the asteroid is not sufficiently bright for the necessary ground-based thermal IR observations. Space-based measurements may be possible using the James Webb Space Telescope (JWST) if the launch schedule is maintained. During the approach phase of AIM, the thermal inertia can be measured with a thermal camera when the spacecraft is a few hundreds of kilometers away from the asteroid or closer. Assuming $\Gamma = 700$ J m^{-2} s$^{-0.5}$ K^{-1}, a value very similar to that of Itokawa, and that there are no librations in Didymoon's 1:1 spin–orbit resonance (synchronous) state, Fig. 6 shows that the primary and the secondary component of the binary system have very different temperature distributions, mainly due to the very different rotation periods of the two bodies.

Interestingly, if the pole of the mutual orbit is parallel to that of the heliocentric orbit, Didymoon's hemisphere facing the primary component will be periodically subject to solar eclipses. The influence of eclipses on the temperature distribution of binary asteroids was noted in the case of the eclipsing binary Patroclus (Müller et al., 2010). In the case of Didymos, note the rapid decrease of the temperature occurs nearly at local midday (180°). Due to repeated solar eclipses, the temperature of the hemisphere facing the primary also has lower temperatures than non-eclipsed areas. This is due to lower-than-average insolation.

Please cite this article in press as: Michel, P., et al. Science case for the Asteroid Impact Mission (AIM): A component of the Asteroid Impact & Deflection Assessment (AIDA) mission. Adv. Space Res. (2016), http://dx.doi.org/10.1016/j.asr.2016.03.031

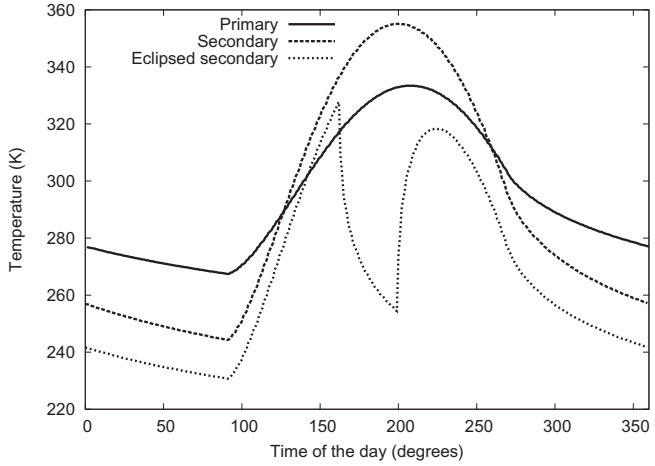

Fig. 6. Equatorial temperatures as a function of time of day (measured in degrees) at the perihelion distance ($q \sim 1.01338$ AU) for the primary, Didymoon, and for an area on Didymoon subject to solar eclipses caused by the primary. This area is located at the "sub-primary" point of Didymoon, i.e., at the point on Didymoon's surface closest to the primary. Local noon occurs at 180°. The bold dashed curve is for the far (uneclipsed) side of Didymoon and the thin dashed curve is for its near (eclipsed) side. The bolometric Bond albedo is calculated to be 0.059, resulting from the geometric visible albedo of 0.15 and an assumed G-value of 0.15.

It is known that rapid temperature variations (Alí-Lagoa et al., 2015) can enhance the effect of thermal surface fracturing (Delbò et al., 2014), likely causing potential variations of the surface thermal inertia. It was noted that the thermal inertia of binary NEAs is different from the thermal inertia of non-binary asteroids of the same population (Delbò et al., 2011). Note also that the eclipsed hemisphere has two thermal cycles every 11.92 h, instead of one. AIM observations of the regolith properties of Didymoon will help to clarify how these different processes work and how they manifest as measurable surface properties.

5.2.4. Environment between the two components

In addition to the two main components of the binary, the possible existence of dust and boulders evolving between them must be assessed. In the context of identified binary formation mechanisms through YORP spin-up, during the secondary formation, mass transfer from one body to the other can happen. However, once the secondary is formed and when it is stabilized, which results in its rotation state being spin-locked, then no major mass transfer is expected to occur. Didymos is now assumed to be in this state.

In fact, as indicated in Section 5.2.1, the case of Didymos is very interesting. Didymos's primary is one of the largest of the *fast spinners*. The tidal pull of Didymoon may create additional perturbations known as *tidal saltation* (Harris et al., 2009). So long as the surface speed is less than the escape speed, which is the case for Didymos' primary, a lifted particle will not escape, but will orbit the body for a time that needs further study to be determined. It may be that the long-term fate of a lofted particle is to join the secondary or to rejoin the primary at a different location.

In general, all asteroids with a spherical shape spinning at angular rates between $\omega = (4\pi\rho G/3)^{1/2}$ and $(8\pi\rho G/3)^{1/2}$, where ρ is the bulk density and G the gravitational constant, can be expected to have at least temporary orbiting debris. The fate of those debris is complicated, but must be assessed if they are present as it may influence the operations and safety of an observing spacecraft. However, once the shape of the primary deviates from a sphere, the limits depend not only on ρ but also on the shape/ellipticity of the primary, e.g., the more oblate it is (up to a maximum oblateness that depends on the details of the exact shape), the faster it can rotate and still hold onto material. Thus the ω bounds become larger than for the pure sphere case.

Note that asteroids spinning faster than the upper limit will have no coarse surface regolith (but fine dust may have enough cohesion to remain on the surface; see Gundlach and Blum, 2015). Those with spins between the limits may have regolith only on parts of the surface.

The survival time of small μm-sized dust particles that lift off the primary is very short due to radiation forces. Preliminary numerical simulations of the system dynamics show that particles that leave the surface land again on the surface itself, sometimes at different latitudes, and this process may go on indefinitely. This could serve as a mechanism that causes continuous dust production in close proximity to the primary. However, it is reasonable to assume that dust will not be a threat for the mission to Didymoon (although shutters for the optical systems, including the camera, may be envisaged, especially in the framework of AIDA).

5.2.5. Possible Yarkovsky drift (and implications for thermal inertia)

In recent years, the densities of several NEAs have been derived by comparing measurements of the rate of change of the orbital semi-major axis da/dt due to the Yarkovsky effect with model predictions of the same observable, the latter being dependent on the size, shape, pole direction, and rotation rate of the asteroid as well as the value of the thermal inertia and the object's bulk density (Rozitis et al., 2013; Chesley et al., 2014; Rozitis and Green, 2014).

In the case of Didymos, in principle the same approach could be used to derive the value of the thermal inertia, assuming that all other parameters are known. In fact, this is the only way to derive this parameter without direct thermal infrared observations.

5.3. Framework of AIDA and the DART impact

5.3.1. Change in physical properties of the secondary

The impact will produce a crater on Didymoon. Its size and morphology highly depend on the sub-surface structure and mechanical properties of Didymoon. Numerical simulations of hypervelocity impacts with a 3D Smoothed

Please cite this article in press as: Michel, P., et al. Science case for the Asteroid Impact Mission (AIM): A component of the Asteroid Impact & Deflection Assessment (AIDA) mission. Adv. Space Res. (2016), http://dx.doi.org/10.1016/j.asr.2016.03.031

Particle Hydrodynamics (SPH) hydrocode using the impact conditions of DART and assuming a porous structure of Didymoon have been performed. They indicate that the diameter of the crater may be of the order of a few to 10–15 m, depending on the assumed structure (see Cheng et al. (2016) for DART impact conditions and more details). Large-scale restructuring is unlikely to occur given the energy regime of the impact event, which is orders of magnitude below the catastrophic disruption impact energy threshold at Didymoon' size, despite its rather low gravitational binding energy. On the other hand, regolith displacement may occur in the vicinity of the impact point and crater, due to the very low gravity of the asteroid. Even small seismic waves may cause displacement or lift-off of loose material. However, there are no reliable existing tools and knowledge to quantify these effects.

5.3.2. Change in dynamical properties of Didymos

The dynamical properties of the system will be affected by the impact. In particular, the orbit of Didymoon around the primary will be modified, as might its rotational properties. Assuming a porous structure, the so-called β factor (the momentum enhancement, defined as the sum of the momentum of the projectile and the momentum of the ejecta in the opposite direction to the impact, normalized by the momentum of the projectile) is 1.4–1.5 based on SPH simulations (Jutzi and Michel, 2014). Other estimates for the β factor (see Cheng et al., 2016) give a range between 1.3 (resulting in a ΔV of 0.52 mm/s) and 4.1 (ΔV of 1.42 mm s^{-1}), for vertical impacts, depending on the assumed internal structure (assuming a 300 kg spacecraft impacting at 6.25 km s^{-1}). Note that these estimates do not account for the effect of the target's rotation on the outcome, which should be tiny as Didymoon is spin-locked. This transfer of momentum will lead to a change in speed (on the order of 0.4 mm/s assuming $\beta = 1$), which in turn will lead to a change in the orbital period of Didymoon around the primary. This change (up to a few minutes) can be measured to within 10% by ground-based observatories and to much higher precision by AIM.

5.3.3. Environment between and around the two components due to impact ejecta

The fate of ejecta produced by the DART impact is an important outcome of the impact event, which has implications on the safety and operations for an observing spacecraft and which also contributes to our better understanding of the impact process. The exact size distribution of the ejecta is still an open question as it depends strongly on the physical properties of Didymoon's upper surface layers. In order to provide some indication of potential safe positions for the spacecraft, we have started to investigate the fate of the ejecta, taking as initial conditions the outcome (ejecta masses/sizes and velocities) expected from the DART impact based on scaling laws and numerical simulations, assuming various kinds of surface properties. Typically, the size distribution of ejecta follows a power-law and given the size of the DART impact event, ejecta whose sizes range from several centimeters to dust are expected. A force balance analysis shows that solar radiation pressure (for relevant ejecta sizes) and solar tides are the dominant perturbations, in addition to the gravitational environment of the binary. The fate of ejecta at the large-size end of the size distribution, which pose the greatest risk to a spacecraft, accounting for all the relevant perturbations, is the subject of a future paper.

Regarding dust ejecta, it is already clear that a significant amount of small particles (1 μm–1 cm) will be ejected. Tails of dust grains have been observed for several asteroids recently impacted or disrupted, such as P/2010 A2 (Jewitt et al., 2010; Snodgrass et al., 2009) and 596 Scheila (Bodewits et al., 2014). Such a debris cloud is typically ejected at relatively low speed and lingers around the asteroid for periods ranging from days to months. These small debris may also be hazardous to the spacecraft, and therefore must be accounted for in our simulations. We considered the fate of very small ejecta (micron- to cm-size particles) by modeling their trajectories with the cometary tail/jets code COSSIM (Vincent et al., 2010). The motion of dust grains in this size range is controlled by the competition between solar gravity and solar radiation pressure, both forces acting in opposite directions and varying with inverse-square distance from the Sun (Finson and Probstein, 1968). The ejection velocity of these particles is not obtained by impact simulations, due to a resolution limit (minimum grain size) of a few cm, so the worst-case scenario was assumed, i.e., the dust grains are ejected at slightly above the escape speed of the Didymos system ($\sim$1 m s^{-1}).

The current mission scenario foresees that the spacecraft will move to a safe distance of 100 km around the time of the impact, and will remain there until all debris have left the system. We modeled the expansion of a dust cloud as described above and calculated the time needed for the particles to escape this safety sphere, for different size ranges (Table 6).

We found that in this regime dust grains smaller than 100 μm will escape in a few hours. Larger grains (1 mm to 10 cm), however, are likely to stay close to the asteroid much longer, up to one month after the impact. Such a slow escape has actually been observed in the case of asteroid P/2010 A2 (Snodgrass et al., 2009), which presented a dust tail interpreted as the result of an impact by a 5-meter-diameter projectile. The larger grains in the ejecta

Table 6
Time after the impact at which impact ejecta in different size-ranges escape the spatial volume separating the asteroid from the spacecraft located at a distance of 100 km.

Ejecta diameter	Time after impact
1–10 μm	6 h
10–100 μm	1 day
0.1–1 mm	3 days
1–10 mm	10 days
1–10 cm	>30 days

Please cite this article in press as: Michel, P., et al. Science case for the Asteroid Impact Mission (AIM): A component of the Asteroid Impact & Deflection Assessment (AIDA) mission. Adv. Space Res. (2016), http://dx.doi.org/10.1016/j.asr.2016.03.031

cloud (diameter >mm) remained detectable from Earth more than one year after the event, still in the vicinity of their parent body.

A future step in our modeling will be to account for the complexity of a binary system, where the revolution of the two bodies around their barycenter may actually help to constrain dust grains to specific trajectories, rather than the simpler spherical expansion we have used here. Because most of the cloud will be expanding in the anti-solar direction, it may also be possible to design orbits maintaining trajectories on the day side of the system, where the dust density is expected to be much lower. This would allow AIM to achieve closer distances to Didymoon soon after the impact.

6. Conclusions

AIDA is a joint cooperation between European and US space agencies that consists of two separate and independent spacecraft, AIM and DART. Until early fall 2016, AIM will be in Phase A/B1 at ESA and DART will be in Phase A at NASA. If the mission is then approved for launch, both spacecraft will be launched independently in 2020 for an arrival in 2022 to the binary near-Earth asteroid Didymos, to assess the possibility of deflecting an asteroid by using a kinetic impactor. The AIM spacecraft will be the first probe that will characterize a binary asteroid, including the surface, subsurface, and internal structure of its smaller component (its main target) and possibly its primary. It will also deploy a few CubeSats and a small lander, allowing us to improve our understanding of the surface response of a low-gravity body. With DART, AIDA will be the first fully documented hypervelocity impact experiment on a small asteroid, in the size range of interest for planetary defense. Implications of this knowledge for Solar System science as well as impact mitigation are enormous, and we can reasonably expect that big surprises, a typical outcome of Solar System space missions, are waiting for us.

Acknowledgments

The authors acknowledge support from ESA and NASA. The work of P.P. and P.S. was supported by the Grant Agency of the Czech Republic, Grant 15-07193S.

References

Alí-Lagoa, V., Delbò, M., Libourel, G., 2015. Rapid temperature changes and the early activity on comet 67P/Churyumov–Gerasimenko. Astrophys. J. 810, L22. http://dx.doi.org/10.1088/2041-8205/810/2/L22.

Barnouin, O.S., Cheng, A.F., Mukai, T., Abe, S., Hirata, N., Nakamura, R., Gaskell, R.W., Saito, J., Clark, B.E., 2008. Small-scale topography of 25143 Itokawa from the Hayabusa laser altimeter. Icarus 198, 108–124.

Binzel, R.P., Perozzi, E., Rivkin, A.S., Rossi, A., Harris, A.W., Bus, S.J., Valsecchi, G.B., Slivan, S.M., 2004. Dynamical and compositional assessment of near-Earth object mission targets. Meteorit. Planet. Sci. 39, 351–366. http://dx.doi.org/10.1111/j.1945-5100.2004.tb00098.x.

Bodewits, D., Vincent, J.-B., Kelley, M.S.P., 2014. Scheila's scar: direct evidence of impact surface alteration on a primitive asteroid. Icarus 229, 190–195. http://dx.doi.org/10.1016/j.icarus.2013.11.003.

Britt, D.T., Yeomans, D., Housen, K., Consolmagno, G., 2002. Asteroid density. Porosity Struct. Asteroids III, 485–500.

Brown, P.G., Assink, J.D., Astiz, L., Blaauw, R., Boslough, M.B., Borovička, J., Brachet, N., Brown, D., Campbell-Brown, M., Ceranna, L., Cooke, W., de Groot-Hedlin, C., Drob, D.P., Edwards, W., Evers, L.G., Garces, M., Gill, J., Hedlin, M., Kingery, A., Laske, G., Le Pichon, A., Mialle, P., Moser, D.E., Saffer, A., Silber, E., Smets, P., Spalding, R.E., Spurný, P., Tagliaferri, E., Uren, D., Weryk, R.J., Whitaker, R., Krzeminski, Z., 2013. A 500-kiloton airburst over Chelyabinsk and an enhanced hazard from small impactors. Nature 503, 238–241. http://dx.doi.org/10.1038/nature12741.

Campo, A., Bagatin, J.-M., Petit Farinella, P., 2001. How many rubble piles are in the asteroid belt? Icarus 149, 198–209. http://dx.doi.org/10.1006/icar.2000.6531.

Canup, R.M., 2012. Forming a Moon with an Earth-like composition via a giant impact. Science 338, 1052–1055. http://dx.doi.org/10.1126/science.1226073.

Cheng, A.F., Atchison, J., Kantsiper, B., Rivkin, A.S., Stickle, A., Reed, C., Galvez, A., Carnelli, I., Michel, P., Ulamec, S., 2015. Asteroid impact & deflection assessment mission. Acta Astronaut. 115, 262–269. http://dx.doi.org/10.1016/j.actaastro.2015.05.021.

Cheng, A.F., Michel, P., Jutzi, M., Rivkin, A.S., Stickle, A., Barnouin, O., Ernst, C., Atchison, J., Pravec, P., Richardson, D., 2016. Asteroid impact & deflection assessment mission: kinteic impactor. Planet. Space Sci. 99, 27–35.

Chesley, S.R., Farnocchia, D., Nolan, M.C., Vokrouhlický, D., Chodas, P.W., Milani, A., Spoto, F., Rozitis, B., Benner, L.A.M., Bottke, W.F., Busch, M.W., Emery, J.P., Howell, E.S., Lauretta, D.S., Margot, J.-L., Taylor, P.A., 2014. Orbit and bulk density of the OSIRIS-REx target asteroid (101955) Bennu. Icarus 235, 5–22. http://dx.doi.org/10.1016/j.icarus.2014.02.020.

Ciarletti, V., Corbel, C., Plettemeier, D., Cais, P., Clifford, S.M., Hamran, P.E., 2011. WISDOM GPR designed for shallow and high-resolution sounding of the martian subsurface. Proc. IEEE 99, 824–836. http://dx.doi.org/10.1109/JPROC.2010.2100790.

Consolmagno, G., Britt, D., Macke, R., 2008. The significance of meteorite density and porosity. Chem. der Erde/Geochem. 68, 1–29. http://dx.doi.org/10.1016/j.chemer.2008.01.003.

Ćuk, M., Stewart, S.T., 2012. Making the Moon from a fast-spinning Earth: a giant impact followed by resonant despinning. Science 338, 1047–1052. http://dx.doi.org/10.1126/science.1225542.

Delbò, M., Walsh, K., Mueller, M., Harris, A.W., Howell, E.S., 2011. The cool surfaces of binary near-Earth asteroids. Icarus 212, 138–148. http://dx.doi.org/10.1016/j.icarus.2010.12.011.

Delbò, M., Libourel, G., Wilkerson, J., Murdoch, N., Michel, P., Ramesh, K.T., Ganino, C., Verati, C., Marchi, S., 2014. Thermal fatigue as the origin of regolith on small asteroids. Nature 508, 233–236. http://dx.doi.org/10.1038/nature13153.

Delbò, M., Mueller, M., Emery, J.P., Rozitis, B., Capria, M.T., 2015. Thermophysical modeling of asteroid surfaces. In: Michel, P., DeMeo, F., Bottke, W.F. (Eds.), Asteroids IV. Univ. Arizona Press, Tucson, pp. 107–128.

de León, J., Licandro, J., Serra-Ricart, M., Pinilla-Alonso, N., Campins, H., 2010. Observations, compositional, and physical characterization of near-Earth and Mars-crosser asteroids from a spectroscopic survey. Astron. Astrophys. 517, A23. http://dx.doi.org/10.1051/0004-6361/200913852.

Duev, D.A., Molera Calvés, G., Pogrebenko, S.V., Gurvits, L.I., Cimó, G., Bocanegra Bahamon, T., 2012. Spacecraft VLBI and doppler tracking: algorithms and implementation. Astron. Astrophys. 541, A43. http://dx.doi.org/10.1051/0004-6361/201218885.

Fang, J., Margot, J.-L., 2012. Near-Earth binaries and triples: origin and evolution of spin-orbital properties. Astron. J. 143, 24. http://dx.doi.org/10.1088/0004-6256/143/1/24.

Finson, M.L., Probstein, R.F., 1968. A theory of dust comets. II. Results for comet arend-roland. Astrophys. J. 154, 353–380. http://dx.doi.org/10.1086/149762.

Fujiwara, A., Kawaguchi, J., Yeomans, D.K., Abe, M., Mukai, T., Okada, T., Saito, J., Yano, H., Yoshikawa, M., Scheeres, D.J., Barnouin-Jha, O., Cheng, A.F., Demura, H., Gaskell, R.W., Hirata, N., Ikeda, H., Kominato, T., Miyamoto, H., Nakamura, A.M., Nakamura, R., Sasaki, S., Uesugi, K., 2006. The rubble-pile asteroid itokawa as observed by hayabusa. Science 312, 1330–1334. http://dx.doi.org/10.1126/science.1125841.

Gaskell, R.W., Barnouin-Jha, O.S., Scheeres, D.J., Konopliv, A.S., Mukai, T., Abe, S., Saito, J., Ishiguro, M., Kubota, T., Hashimoto, T., Kawaguchi, J., Yoshikawa, M., Shirakawa, K., Kominato, T., Hirata, N., Demura, H., 2008. Characterizing and navigating small bodies with imaging data. Meteorit. Planet. Sci. 43, 1049–1061.

Gundlach, B., Blum, J., 2013. A new method to determine the grain size of planetary regolith. Icarus 223, 479–492. http://dx.doi.org/10.1016/j.icarus.2012.11.039.

Gundlach, B., Blum, J., 2015. Regolith grain size and cohesive strength of near-Earth asteroid (29075) 1950 DA. Icarus 257, 126–129. http://dx.doi.org/10.1016/j.icarus.2015.04.032.

Harris, A.W., Fahnestock, E.G., Pravec, P., 2009. On the shapes and spins of rubble pile asteroids. Icarus, 310–318. http://dx.doi.org/10.1016/j.icarus.2008.09.012.

Herique, A., 2015. A direct observation the asteroid's structure from deep interior to regolith: why and how do it? LPI Contrib. 1829, 6018.

Holsapple, K.A., 1993. The scaling of impact processes in planetary sciences. Annu. Rev. Earth Planet. Sci. 21, 333–373. http://dx.doi.org/10.1146/annurev.ea.21.050193.002001.

Holsapple, K.A., Housen, K.R., 2012. Momentum transfer in asteroid impacts. I. Theory and scaling. Icarus 221, 875–887. http://dx.doi.org/10.1016/j.icarus.2012.09.022.

Holsapple, K.A., Schmidt, R.M., 1987. Point source solutions and coupling parameters in cratering mechanics. J. Geophys. Res. 92, 6350–6376. http://dx.doi.org/10.1029/JB092iB07p06350.

Holsapple, K., Giblin, I., Housen, K., Nakamura, A., Ryan, E., 2002. Asteroid impacts: laboratory experiments and scaling laws. In: Bottke, W.F., Cellino, A., Paolicchi, P., Binzel, R.P. (Eds.), Asteroids III. Univ. Arizona Press, Tucson, pp. 443–462.

Hörz, F., Cintala, M., 1997. Impact experiments related to the evolution of planetary regoliths. Meteorit. Planet. Sci. 32, 179–209. http://dx.doi.org/10.1111/j.1945-5100.1997.tb01259.x.

Jacobson, S.A., Scheeres, D.J., 2011. Dynamics of rotationally fissioned asteroids: source of observed small asteroid systems. Icarus 214, 161–178. http://dx.doi.org/10.1016/j.icarus.2011.04.009.

Jaumann, R., Bibring, J.-P., Glassmeier, K.-H., Grott, M., Ho, T.-M., Ulamec, S., Schmitz, N., Auster, H.-U., Biele, J., Kuninaka, H., Okada, T., Yoshikawa, M., Watanabe, S., Fujimoto, M., Spohn, T., 2013. A mobile asteroid surface scout (MASCOT) for the Hayabusa 2 mission to 1999 JU3: the scientific approach. In: Lunar and Planetary Science Conference, Lunar and Planetary Science Conference, vol. 44, p. 1500.

Jewitt, D., Weaver, H., Agarwal, J., Mutchler, M., Drahus, M., 2010. A recent disruption of the main-belt asteroid P/2010A2. Nature 467, 817–819. http://dx.doi.org/10.1038/nature09456.

Jutzi, M., Michel, P., 2014. Hypervelocity impacts on asteroids and momentum transfer I. Numerical simulations using porous targets. Icarus 229, 247–253. http://dx.doi.org/10.1016/j.icarus.2013.11.020.

Jutzi, M., Holsapple, K.H., Wünneman, K., Michel, P., 2015. Modeling asteroid collisions and impact processes. In: Michel, P., DeMeo, F., Bottke, W.F. (Eds.), Asteroids IV. Univ. Arizona Press, Tucson, pp. 679–699.

Kofman, W., 2007. Radar techniques to study subsurfaces and interiors of the solar system objects, AGU Fall Meeting Abstracts, B1.

Kofman, W., Herique, A., Barbin, Y., Barriot, J.-P., Ciarletti, V., Clifford, S., Edenhofer, P., Elachi, C., Eyraud, C., Goutail, J.-P., Heggy, E., Jorda, L., Lasue, J., Levasseur-Regourd, A.-C., Nielsen, E., Pasquero, P., Preusker, F., Puget, P., Plettemeier, D., Rogez, Y., Sierks, H., Statz, Svedhem, H., Williams, I., Zine, S., Van Zyl, J., 2015. Properties of the 67P/Churyumov–Gerasimenko interior revealed by CONSERT radar. Science 349 (2), 020639. http://dx.doi.org/10.1126/science.aab0639.

Konopliv, A.S., Miller, J.K., Owen, W.M., Yeomans, D.K., Giorgini, J. D., Garmier, R., Barriot, J.-P., 2002. A global solution for the gravity field. Rotation, landmarks, and ephemeris of eros. Icarus 160, 289–299. http://dx.doi.org/10.1006/icar.2002.6975.

Koschny, D., Drolshagen, G., 2015. Activities in Europe related to the mitigation of the threat from near-Earth objects. Adv. Space Res. 56, 549–556. http://dx.doi.org/10.1016/j.asr.2015.03.027.

Margot, J.-L., Pravec, P., Taylor, P., Carry, B., Jacobson, S., 2015. Asteroid systems: binaries, triples, and pairs. In: Michel, P., DeMeo, F., Bottke, W.F. (Eds.), Asteroids IV. Univ. Arizona Press, Tucson, pp. 355–374.

Mazrouei, S., Daly, M.G., Barnouin, O.S., Ernst, C.M., DeSouza, I., 2014. Block distributions on Itokawa. Icarus 229, 181–189.

Michel, P., 2013. Physical properties of near-Earth objects that inform mitigation. Acta Astronaut. 90, 6–13. http://dx.doi.org/10.1016/j.actaastro.2012.07.022.

Michel, P., Benz, W., Tanga, P., Richardson, D.C., 2001. Collisions and gravitational reaccumulation: forming asteroid families and satellites. Science 294, 1696–1700. http://dx.doi.org/10.1126/science.1065189.

Michel, P., DeMeo, F., Bottke, W.F., 2015. Asteroids: recent advances and new perspectives. In: Michel, P., DeMeo, F., Bottke, W.F. (Eds.), Asteroids IV. Univ. Arizona Press, Tucson, pp. 341–354.

Müller, M., Marchis, F., Emery, J.P., Harris, A.W., Mottola, S., Hestroffer, D., Berthier, J., di Martino, M., 2010. Eclipsing binary trojan asteroid patroclus: thermal inertia from Spitzer observations. Icarus 205, 505–515. http://dx.doi.org/10.1016/j.icarus.2009.07.043.

Murdoch, N., Sánchez, P., Schwartz, S.R., Miyamoto, H., 2015. Asteroid surface geophysics. In: Michel, P., DeMeo, F., Bottke, W.F. (Eds.), Asteroids IV. Univ. Arizona Press, Tucson, pp. 767–792.

Naidu, S.P., Margot, J.-L., 2015. Near-Earth asteroid satellite spins under spin-orbit coupling. Astron. J. 149 (80). http://dx.doi.org/10.1088/0004-6256/149/2/80.

Piqueux, S., Christensen, P.R., 2009a. A model of thermal conductivity for planetary soils: 1. Theory for unconsolidated soils. J. Geophys. Res. (Planets) 114. http://dx.doi.org/10.1029/2008JE003308, E09005.

Piqueux, S., Christensen, P.R., 2009b. A model of thermal conductivity for planetary soils: 1. Theory for cemented soils. J. Geophys. Res. (Planets) 114. http://dx.doi.org/10.1029/2008JE003309, E09006.

Pravec, P., Benner, L.A.M., Nolan, M.C., Kusnirak, P., Pray, D., Giorgini, J.D., Jurgens, R.F., Ostro, S.J., Margot, J.-L., Magri, C., Grauer, A., Larson, S., 2003. (65803) 1996 GT. IAU Circ. 8244, 2.

Pravec, P., Scheirich, P., Kušnirák, P., Šarounová, L., Mottola, S., Hahn, G., Brown, P., Esquerdo, G., Kaiser, N., Krzeminski, Z., Pray, D.P., Warner, B.D., Harris, A.W., Nolan, M.C., Howell, E.S., Benner, L.A. M., Margot, J.-L., Galád, A., Holliday, W., Hicks, M.D., Krugly, Y. N., Tholen, D., Whiteley, R., Marchis, F., DeGraff, D.R., Grauer, A., Larson, S., Velichko, F.P., Cooney, W.R., Stephens, R., Zhu, J., Kirsch, K., Dyvig, R., Snyder, L., Reddy, V., Moore, S., Gajdoš, Š., Világi, J., Masi, G., Higgins, D., Funkhouser, G., Knight, B., Slivan, S., Behrend, R., Grenon, M., Burki, G., Roy, R., Demeautis, C., Matter, D., Waelchli, N., Revaz, Y., Klotz, A., Rieugné, M., Thierry, P., Cotrez, V., Brunetto, L., Kober, G., 2006. Photometric survey of binary near-Earth asteroids. Icarus 181, 63–93. http://dx.doi.org/10.1016/j.icarus.2005.10.014.

Pravec, P., Harris, A.W., Kušnirák, P., Galád, A., Hornoch, K., 2012. Absolute magnitudes of asteroids and a revision of asteroid albedo estimates from WISE thermal observations. Icarus 221, 365–387. http://dx.doi.org/10.1016/j.icarus.2012.07.026.

Pravec, P., Scheirich, P., Kušnirák, P., Hornoch, K., Galád, A., Naidu, S. P., Pray, D.P., Világi, J., Gajdoš, Š., Kornoš, L., Krugly, Y.N., Cooney, W.R., Gross, J., Terrell, D., Gaftonyuk, N., Pollock, J., Husárik, M., Chiorny, V., Stephens, R.D., Durkee, R., Reddy, V., Dyvig, R., Vraštil, J., Žižka, J., Mottola, S., Hellmich, S., Oey, J., Benishek, V., Kryszczyńska, A., Higgins, D., Ries, J., Marchis, F.,

Baek, Macomber, B., Inasaridze, R., Kvaratskhelia, O., Ayvazian, V., Rumyantsev, V., Masi, G., Colas, F., Lecacheux, J., Montaigut, R., Leroy, A., Brown, P., Krzeminski, Z., Molotov, I., Reichart, D., Haislip, J., LaCluyze, A., 2012. Binary asteroid population. 3. Secondary rotations and elongations. Icarus 267, 267–295. http://dx.doi.org/10.1016/j.icarus.2015.12.019.

Reufer, A., Meier, M.M.M., Benz, W., Wieler, R., 2012. A hit-and-run giant impact scenario. Icarus 221, 296–299. http://dx.doi.org/10.1016/j.icarus.2012.07.021.

Richardson, J.E., Melosh, J.H., 2013. An examination of the deep impact collision site on comet tempel 1 via stardust-NExT: placing further constraints on cometary surface properties. Icarus 222, 492–501. http://dx.doi.org/10.1016/j.icarus.2012.04.019.

Richardson, D.C., Leinhardt, Z.M., Melosh, H.J., Bottke Jr., W.F., Asphaug, E., 2002. Gravitational aggregates: evidence and evolution. In: Bottke, W.F., Jr., Cellino, A., Paolicchi, P., Binzel, R.P. (Eds.), Asteroids III. Univ. Arizona Press, Tucson, pp. 501–515.

Rosenblatt, P., Dehant, V., 2010. Mars geodesy, rotation and gravity. Res. Astron. Astrophys. 10, 713–736. http://dx.doi.org/10.1088/1674-4527/10/8/002.

Rozitis, B., Green, S.F., 2014. Physical characterisation of near-Earth asteroid (1620) geographos. Reconciling radar and thermal-infrared observations. Astron. Astrophys. 568, A43.

Rozitis, B., Duddy, S.R., Green, S.F., Lowry, S.C., 2013. A thermophysical analysis of the (1862) Apollo Yarkovsky and YORP effects. Astron. Astrophys. 555, A20. http://dx.doi.org/10.1051/0004-6361/201321659.

Rozitis, B., Maclennan, E., Emery, J.P., 2014. Cohesive forces prevent the rotational breakup of rubble-pile asteroid (29075) 1950 DA. Nature 512, 174–176. http://dx.doi.org/10.1038/nature13632.

Scheeres, D.J., Hartzell, C.M., Sánchez, P., Swift, M., 2010. Scaling forces to asteroid surfaces: the role of cohesion. Icarus 210, 968–984. http://dx.doi.org/10.1016/j.icarus.2010.07.009.

Scheirich, P., Pravec, P., 2009. Modeling of lightcurves of binary asteroids. Icarus 200, 531–547. http://dx.doi.org/10.1016/j.icarus.2008.12.001.

Schultz, P.H., Hermalyn, B., Veverka, J., 2013. The deep impact crater on 9P/Tempel-1 from stardust-NExT. Icarus 222, 502–515. http://dx.doi.org/10.1016/j.icarus.2012.06.018.

Snodgrass, C., Tubiana, C., Vincent, J.-B., Sierks, H., Hviid, S., Moissi, R., Boehnhardt, H., Barbieri, C., Koschny, D., Lamy, P., Rickman, H., Rodrigo, R., Carry, B., Lowry, S.C., Laird, R.J.M., Weissman, P. R., Fitzsimmons, A., Marchi, S.OSIRIS Team, 2009. A collision in 2009 as the origin of the debris trail of asteroid P/2010A2. Nature 467 (2010), 814–816. http://dx.doi.org/10.1038/nature09453.

Ulamec, S., Biele, J., Bousquet, P.-W., Gaudon, P., Geurts, K., Ho, T.-M., Krause, C., Lange, C., Willnecker, R., Witte, L., 2014. The Philae, mascot teams, landing on small bodies: from the rosetta lander to MASCOT and beyond. Acta Astronaut. 93, 460–466. http://dx.doi.org/10.1016/j.actaastro.2013.02.007.

Vincent, J.-B., Böhnhardt, H., Lara, L.M., 2010. A numerical model of cometary dust coma structures. Application to comet 9P/Tempel 1. Astron. Astrophys. 512, A60.

Vokrouhlický, D., Bottke, W.F., Chesley, S.R., Scheeres, D., Statler, T., 2015. The Yarkovsky and YORP effects. In: Michel, P., DeMeo, F., Bottke, W.F. (Eds.), Asteroids IV. Univ. Arizona Press, Tucson, pp. 509–531.

Walsh, K.J., Jacobson, S.A., 2015. Formation and evolution of binary asteroids. In: Michel, P., DeMeo, F., Bottke, W.F. (Eds.), Asteroids IV. Univ. Arizona Press, Tucson, 375–393.

Walsh, K.J., Richardson, D.C., Michel, P., 2008. Rotational breakup as the origin of small binary asteroids. Nature 454, 188–191. http://dx.doi.org/10.1038/nature07078.

Walsh, K.J., Richardson, D.C., Michel, P., 2012. Spin-up of rubble-pile asteroids: disruption, satellite formation, and equilibrium shapes. Icarus 220, 514–529. http://dx.doi.org/10.1016/j.icarus.2012.04.029.

Wentworth, C.K., 1922. A scale of grade and class terms for clastic sediments. J. Geol. 30, 377–392. http://dx.doi.org/10.1086/622910.

Please cite this article in press as: Michel, P., et al. Science case for the Asteroid Impact Mission (AIM): A component of the Asteroid Impact & Deflection Assessment (AIDA) mission. Adv. Space Res. (2016), http://dx.doi.org/10.1016/j.asr.2016.03.031